Rakenteiden Mekaniikka (Journal of Structural Mechanics)
Vol. 44, No 3, 2011, pp. 172 – 185

Static instability analysis of an elastic band travelling in the gravitational field

Nikolay Banichuk, Juha Jeronen, Tytti Saksa and Tero Tuovinen

Summary. Static instability analysis is performed for an axially moving elastic band, which is travelling at a constant velocity in a uniform gravitational field between two supports. The buckling of the band is investigated with the help of admitting small transverse deflections. The model of a thin elastic beam (panel) subjected to bending, centrifugal forces and nonhomogeneous tension (including a gravitational term) is used. Buckling analysis and estimation of the critical velocities of elastic instability are based on variational principles and variational inequalities. As a result, explicit formulas for upper and lower limits for critical velocities are found. It is shown analytically that a critical velocity always exists. The critical buckling modes are found, first, by solving the original differential equation directly, and, secondly, by energy minimization. The buckling modes and corresponding critical velocities are found and illustrated with some numerical examples. The gravitational force is shown to have a major effect on the buckled shape, but a minor effect on the critical velocity.

Key words: stability, paper industry, paper, elasticity, gravitation, partial differential equations, optimization

Introduction

Vibrations and stability of axially moving materials, such as strings, beams, membranes and plates, have been studied widely, since such models have various applications in industry, e.g., in paper making or in transmission cables. Stability studies of travelling materials are important, since they yield information on critical transport velocities for machine operation.

In previous studies concerning vibrations of (moving) materials, the effect of gravity has usually been neglected, since its magnitude is minor compared to the magnitude of the axial tension. Recently, Luo and Mote have studied equilibrium of travelling elastic, sagged cables under uniformly distributed loading [10]. For a three-dimensional model, they derived exact, closed-form solutions for the equilibrium configuration and tension distribution of the cables. The present study concentrates on stability of thin, elastic panels and critical velocity estimations.

Vibrations of travelling strings, beams and bands have first been studied by Archibald and Emslie [1], Miranker [11], Swope and Ames [17] Mote [12, 13, 14], Simpson [16], Ulsoy and Mote [18], Chonan [5], Wickert and Mote [21]. These studies focused on free and forced vibrations including the nature of wave propagation in moving media and the effects of axial motion on the eigenfrequencies and eigenmodes. Stability of travelling two-dimensional rectangular membranes and plates have been studied by Ulsoy and Mote [19], Lin and Mote [9], Lin [8], Banichuk et al. [2].

Archibald and Emslie [1] and Simpson [16] studied effects of the axial motion on the eigenfrequencies and eigenfunctions. It was shown that the natural frequency of each mode decreases when the transport speed increases, and that the travelling string and beam both experince divergence instability at a sufficiently high speed. Stability considerations were reviewed by Mote [13].

Recent studies on travelling materials have been performed, e.g., by Shin et al. [15], Wang et al. [20], Frondelius et al. [7], Banichuk et al. [3]. In Shin et al., the out-of-plane vibrations of an axially moving membrane were studied, and it was shown numerically that membrane is stable until a critical velocity, at which statical instability occurs [15]. Wang et al. studied transverse vibrations of axially moving strings [20]. In their study, it was shown using a Hamiltonian approach that for the transverse motion of the string, no instability occurs at the critical velocity, where a steady-state solution exists.

Frondelius et al. [7] and Banichuk et al. [3] studied a travelling band interacting with surrounding fluid and the fluid-web-contact influence on the critical velocity. Banichuk et al. studied the static instability of the travelling band submerged in flowing ideal fluid, and it was found that in presence of fluid the critical divergence speed is much lower than the vacuum solution and the divergence shape also differs from the vacuum case [3].

In the present study, the static instability of an axially moving thin, elastic band is investigated, when the band is travelling in the gravitational field. The investigation is performed in the case where the band is moving parallel to the gravity but it can also be applied to cases in which the direction of motion with respect to the gravity varies, of which several numerical examples are given. Based on variational principles and variational inequalities, explicit estimations for the critical velocity are derived. In the numerical examples, the effects of the gravity are visualised.

The critical transport velocity and the corresponding buckled shape are found numerically by solving directly the original differential equation via the Fourier–Galerkin method. Secondly, they are solved by minimizing a functional corresponding to the energy. The obtained nonlinear optimization problem is solved numerically using the Rayleigh–Ritz method.

Basic relations

We consider an elastic band, travelling at a constant velocity between two supports parallel to a uniform gravitational field (Earth's) in a rectangular coordinate system. We study the transverse displacement w of the band assuming that the displacement is cylindrical, i.e., the displacement does not vary in the cross section (in the y direction). The distance between the two supports is constant, denoted by ℓ.

The transport velocity of the panel is assumed to be a constant, V_0, and the panel is moving along the x axis. The panel is tensioned at the edges, and the tension T depends on the space coordinate x, $T = T(x)$. The standard gravity constant is denoted by g, and the thickness of the panel by h. The panel is assumed to have a constant mass per unit area, m.

The dynamic equation for the transverse displacement of the panel can be written as

$$m\,w_{tt} + 2mV_0\,w_{xt} + mV_0^2\,w_{xx} = T\,w_{xx} + T_x\,w_x - D\,w_{xxxx}\,. \tag{1}$$

Here, D describes the bending rigidity of the panel.

Tension T varies due to the gravity as

$$T(x) = T_0 + mgx\,, \tag{2}$$

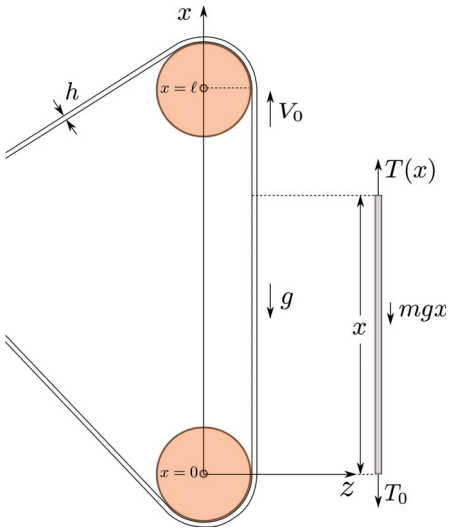

Figure 1. Panel moving in the gravitational field.

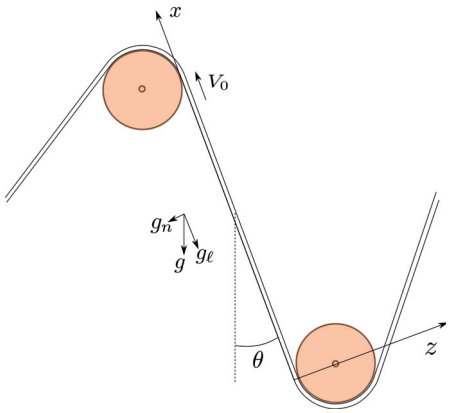

Figure 2. The elastic band moving in a nonvertical direction (inclined with respect to the gravity).

where T_0 is a constant tension at the lower edge of the panel (see Figure 1). Substituting (2) into (1), we obtain

$$m\,w_{tt} + 2mV_0\,w_{xt} + mV_0^2\,w_{xx} = (T_0 + mgx)\,w_{xx} + mg\,w_x - D\,w_{xxxx}\,. \tag{3}$$

In the more general case, where the direction of motion of the band has some nonzero angle θ with respect to the uniform gravitational field, we can perform analogous analysis using the expression

$$T(x) = mgx\cos\theta + T_0 \tag{4}$$

instead of (2), and include the term $mg\sin\theta$ in the right-hand side of (3). See Figure 2.

Buckling analysis

To study the instability of the panel, we perform a buckling analysis. The static form of the dynamic equation (3) is studied as a spectral boundary value problem using simply supported (also known as pinned or hinged) boundary conditions.

Equilibrium for the transverse displacement w is described by the following differential equation

$$mV_0^2\,w_{xx} - (T_0 + mgx)\,w_{xx} - mg\,w_x + D\,w_{xxxx} = 0\,. \tag{5}$$

The boundary conditions are

$$w(0) = w_{xx}(0) = 0, \quad w(\ell) = w_{xx}(\ell) = 0. \tag{6}$$

We represent (5)–(6) in a dimensionless form

$$\left[\frac{V_0^2}{T_0/m} - 1 - \frac{mg\ell}{T_0}x\right] w_{xx} - \frac{mg\ell}{T_0}\, w_x + \frac{D}{\ell^2 T_0}\, w_{xxxx} = 0\,,$$
$$w(0) = w_{xx}(0) = 0\,, \quad w(1) = w_{xx}(1) = 0\,, \tag{7}$$

where $x \in [0,1]$ is the dimensionless coordinate. By defining

$$c_0 := V_0/\sqrt{T_0/m}\,, \tag{8}$$
$$\alpha := \frac{D}{\ell^2 T_0}\,, \tag{9}$$
$$\beta := \frac{mg\ell}{T_0}\,, \tag{10}$$

and substituting (8)–(10) into (7), we obtain

$$\alpha\, w_{xxxx} + (c_0^2 - 1 - \beta x)\, w_{xx} - \beta\, w_x = 0\,, \tag{11}$$
$$w(0) = w_{xx}(0) = 0\,, \quad w(1) = w_{xx}(1) = 0\,. \tag{12}$$

Boundary value problem and variational principle

Consider the boundary value problem (11)–(12). Multiply (11) by a test function v, satisfying the boundary conditions (12) and integrate the obtained equation over $[0,1]$:

$$\alpha \int_0^1 w_{xxxx} v \,\mathrm{d}x + (c_0^2 - 1)\int_0^1 w_{xx} v \,\mathrm{d}x - \beta \int_0^1 x w_{xx} v \,\mathrm{d}x - \beta \int_0^1 w_x v \,\mathrm{d}x = 0\,. \tag{13}$$

Integration by parts yields

$$\int_0^1 w_{xx} v \,\mathrm{d}x = -\int_0^1 w_x v_x \,\mathrm{d}x\,, \qquad \int_0^1 x w_{xx} v \,\mathrm{d}x = -\int_0^1 x w_x v_x \,\mathrm{d}x - \int_0^1 w_x v \,\mathrm{d}x\,,$$
$$\int_0^1 w_{xxxx} v \,\mathrm{d}x = \int_0^1 w_{xx} v_{xx} \,\mathrm{d}x\,. \tag{14}$$

Substitute (14) into (13) to obtain

$$\alpha \int_0^1 w_{xx} v_{xx} \,\mathrm{d}x + (1 - c_0^2)\int_0^1 w_x v_x \,\mathrm{d}x + \beta \int_0^1 x w_x v_x \,\mathrm{d}x = 0\,. \tag{15}$$

Substituting $v = w$ into (15), we finally obtain

$$\alpha \int_0^1 w_{xx}^2 \,\mathrm{d}x + (1 - c_0^2)\int_0^1 w_x^2 \,\mathrm{d}x + \beta \int_0^1 x w_x^2 \,\mathrm{d}x = 0\,. \tag{16}$$

The left hand side of the equation (16) corresponds to the energy of the system. We want to find the minimal velocity c_0, at which equation (16) has a non-trivial solution.

Thus, we resolve c_0^2 from (16), and minimize the other side of the obtained equation. This minimal velocity is the critical velocity for the buckling problem [6], and is obtained from

$$(c_0^*)^2 = \min_{w\in K}\left(1+\alpha\,\frac{\int_0^1 (w_{xx})^2\,\mathrm{d}x}{\int_0^1 (w_x)^2\,\mathrm{d}x}+\beta\,\frac{\int_0^1 x\,(w_x)^2\,\mathrm{d}x}{\int_0^1 (w_x)^2\,\mathrm{d}x}\right), \tag{17}$$

where

$$K=\{w\in C([0,1]) : w(0)=0\,,\quad w(1)=0\}\,. \tag{18}$$

The function w minimizing (17)–(18) is the buckling mode corresponding to the critical velocity c_0^*.

Let us show that the minimization problem (17)–(18) corresponds to the original problem (11)–(12). Denote

$$I(w)=1+\alpha\,\frac{\int_0^1 (w_{xx})^2\,\mathrm{d}x}{\int_0^1 (w_x)^2\,\mathrm{d}x}+\beta\,\frac{\int_0^1 x\,(w_x)^2\,\mathrm{d}x}{\int_0^1 (w_x)^2\,\mathrm{d}x}\,,$$

and

$$I_1(w)=\int_0^1 (w_{xx})^2\,\mathrm{d}x\,,\quad I_2(w)=\int_0^1 (w_x)^2\,\mathrm{d}x\,,\quad I_3(w)=\int_0^1 x(w_x)^2\,\mathrm{d}x\,. \tag{19}$$

It can be easily seen that if $w\not\equiv 0$, then

$$I_1(w)>0\,,\quad I_2(w)>0\,,\quad I_3(w)>0\,.$$

Let w^* be the minimizer of (17)–(18). To prove that w^* satisfies the necessary extremum condition, we derive the Euler equation for w^*. Since w^* is the minimizer, the first variation of $I(w^*)$ is zero, that is

$$\delta I(w^*)=0\,.$$

Notice that

$$\delta I=\frac{1}{I_2}(\alpha\,\delta I_1+\beta\,\delta I_3)-\frac{1}{I_2^2}(\alpha\,I_1+\beta\,I_3)\,\delta I_2\,. \tag{20}$$

As a result from the variation in (20), we obtain

$$\frac{2}{I_2(w^*)}\int_0^1 \left(\alpha w^*_{xxxx}-\beta x w^*_{xx}-\beta w^*_x+(c_0^2-1)w^*_{xx}\right)\delta w\,\mathrm{d}x=0\,, \tag{21}$$

for any function $\delta w\in K$. In addition, w must satisfy the boundary conditions (12). Equation (21) holds for all $\delta w\in K$. Thus, the resulting Euler equation is

$$\alpha w^*_{xxxx}-\beta x w^*_{xx}-\beta w^*_x+(c_0^2-1)w^*_{xx}=0\,,$$

which is (11). In other words, the solution w^* of the minimization problem (17)–(18) is a weak solution of the original problem (11)–(12).

Estimations for the critical velocity

In this section, we derive analytical lower and upper bounds for the critical velocity. We estimate the critical velocity c_0^* corresponding to (11)–(12) given by the relation

$$(c_0^*)^2 = I(w^*) = 1 + \alpha \frac{I_1(w^*)}{I_2(w^*)} + \beta \frac{I_3(w^*)}{I_2(w^*)} . \tag{22}$$

For the lower bound of (22), we obtain

$$(c_0^*)^2 \geq 1 + \alpha \min_{w \in K} \frac{I_1(w)}{I_2(w)} . \tag{23}$$

For the upper bound of (22), we have

$$(c_0^*)^2 \leq 1 + \alpha \frac{I_1(w^a)}{I_2(w^a)} + \beta \frac{I_3(w^a)}{I_2(w^a)} , \tag{24}$$

where w^a is any function in K.

Combining (23) and (24), we can estimate c_0^* as follows:

$$1 + \alpha \min_{w \in K} \frac{I_1(w)}{I_2(w)} \leq (c_0^*)^2 \leq 1 + \alpha \frac{I_1(w^a)}{I_2(w^a)} + \beta \frac{I_3(w^a)}{I_2(w^a)} . \tag{25}$$

To find the lower bound accurately, we solve the minimisation problem

$$\min_{w \in K} \frac{I_1(w)}{I_2(w)} . \tag{26}$$

Problem (26) can be transformed to the following boundary value problem (Euler equation with boundary conditions):

$$\begin{gathered} w_{xxxx} + \lambda\, w_{xx} = 0 \\ w(0) = w_{xx} = 0 , \quad w(1) = w_{xx}(1) = 0 . \end{gathered} \tag{27}$$

Solutions to eigenvalue problem (27) are known to be

$$\begin{aligned} w_k(x) &= A \sin(k\pi x) , \quad k = 1, 2, 3, \ldots , \\ \lambda_k &= (k\pi)^2 . \end{aligned}$$

The normalised solution ($A = 1$) corresponding to the minimum in (26) can be shown to be

$$\begin{aligned} w_{\min}(x) = w_1(x) &= \sin(\pi x) , \\ \lambda_{\min} = \lambda_1 &= \pi^2 . \end{aligned}$$

Inserting w_1 into (19), we obtain

$$\begin{gathered} I_1(w_1) = \pi^2 \int_0^1 \cos^2(\pi x)\, \mathrm{d}x = \frac{\pi^2}{2} , \qquad I_2(w_1) = \int_0^1 \sin^2(\pi x)\, \mathrm{d}x = \frac{1}{2} \\ I_3(w_1) = \int_0^1 x \sin^2(\pi x)\, \mathrm{d}x = \frac{1}{4} . \end{gathered} \tag{28}$$

Choosing $w^a = w_1 \in K$ in (24) and inserting (28) into (25), we obtain the estimate

$$1 + \alpha\, \pi^2 \leq (c_0^*)^2 \leq 1 + \alpha\, \pi^2 + \frac{\beta}{2} . \tag{29}$$

Estimate (29) gives lower and upper bounds for $(c_0^*)^2$. Here, c_0, α and β are defined in (8), (9)–(10).

Numerical solution by the Rayleigh–Ritz and the Fourier–Galerkin methods

The minimization problem was discretized using the Rayleigh-Ritz method and solved using the interior point method. The differential equation was solved via the Fourier-Galerkin method. Both methods were realized in Matlab.

Numerical solution for the minimization problem

Consider the minimization problem (17). Constant one does not effect the location of the optimum and it can be omitted. Divide (17) by constant α. The obtained minimization problem is equivalent to (17):

$$\min_{w\in K}\left[\frac{\int_0^1 (w_{xx})^2\,\mathrm{d}x + a\int_0^1 x\,(w_x)^2\,\mathrm{d}x}{\int_0^1 (w_x)^2\,\mathrm{d}x}\right], \tag{30}$$

where

$$a = \frac{\beta}{\alpha} = \frac{gm\ell^3}{D}\,.$$

The problem (30) has infinite amount of solutions: If w is a solution, then also cw, c is a constant, is a solution. Problem (30) can be solved as [6, p. 273]

$$\begin{aligned}&\min_{w\in K}\int_0^1 (w_{xx})^2\,\mathrm{d}x + a\int_0^1 x\,(w_x)^2\,\mathrm{d}x\\ &\text{subject to }\int_0^1 (w_x)^2\,\mathrm{d}x = 1\,.\end{aligned} \tag{31}$$

In addition, w must satisfy boundary conditions $w(0) = w(1) = 0$. Now, the condition $\int_0^1 (w_x)^2\mathrm{d}x = 1$ sets the absolute value of the constant c mentioned above. Note that the normalization constant, which is now chosen to be one, can be chosen freely.

We discretize (31) using the Rayleigh-Ritz method. We present function w as a series

$$w(x) = \sum_{j=1}^{\infty} v_j\varphi_j(x) \tag{32}$$

in the basis

$$\varphi_j(x) \equiv \sin(j\pi x)\,, \quad x\in[0,1]. \tag{33}$$

The basis (33) fulfills the boundary conditions $w(0) = w(1) = 0$ naturally. We fix a finite positive integer n_0 (number of modes), and approximate (32) with its finite analog

$$w(x) = \sum_{j=1}^{n_0} v_j\varphi_j(x)\,. \tag{34}$$

Inserting (33)–(34) into (31), we obtain

$$\begin{aligned}&\min \quad \mathbf{v}^{\mathrm{T}}\mathbf{A}\mathbf{v} + a\,\mathbf{v}^{\mathrm{T}}\mathbf{B}\mathbf{v}\\ &\text{subject to} \quad \mathbf{v}^{\mathrm{T}}\mathbf{C}\mathbf{v} - 1 = 0\,,\end{aligned} \tag{35}$$

where $\mathbf{v} = (v_1,\ldots,v_{n_0})^{\mathrm{T}} \in \mathbb{R}^{n_0}$.

The elements of the matrices in (35) can be found analytically. They are

$$
\begin{aligned}
A_{ij} &:= \int_0^1 (\varphi_j)_{xx} (\varphi_i)_{xx} \, \mathrm{d}x = \frac{j^4\pi^4}{2}\delta_{ij} \,, \\
B_{ij} &:= \int_0^1 x (\varphi_j)_x (\varphi_i)_x \, \mathrm{d}x = -\int_0^1 x (\varphi_j)_{xx} \varphi_i \, \mathrm{d}x - \int_0^1 (\varphi_j)_x \varphi_i \, \mathrm{d}x = -E_{ij} - D_{ij} \,, \\
C_{ij} &:= \int_0^1 (\varphi_j)_x (\varphi_i)_x \, \mathrm{d}x = \frac{j^2\pi^2}{2}\delta_{ij} \,, \\
D_{ij} &:= \int_0^1 (\varphi_j)_x \varphi_i \, \mathrm{d}x = \begin{cases} 0 & , \quad i = j \\ \frac{ij\left[(-1)^{i+j}-1\right]}{j^2-i^2} & , \quad i \neq j \end{cases} \,, \\
E_{ij} &:= \int_0^1 x (\varphi_j)_{xx} \varphi_i \, \mathrm{d}x = \begin{cases} -\frac{j^2\pi^2}{4} & , \quad i = j \\ -\frac{2ij^3\left[(-1)^{i+j}-1\right]}{[i-j]^2[i+j]^2} & , \quad i \neq j \end{cases} \,,
\end{aligned} \tag{36}
$$

where δ_{ij} is the Kronecker delta.

The discretized problem (35) is a nonlinear optimization problem with a nonlinear objective function and a nonlinear constraint. The optimization problem variable is vector $\mathbf{v}$. Note that the size of the problem depends on n_0. Note also that the boundary conditions are included in matrices $\mathbf{A}$, $\mathbf{B}$ ja $\mathbf{C}$.

Numerical solution of the differential equation

The numerical solution of the original boundary value problem (5)–(6) was performed by using the Fourier–Galerkin method.

Define

$$\lambda := 1 - c_0^2 \,. \tag{37}$$

Consider the dimensionless problem (11)–(12). Eigenvalue problem for the eigenvalue-eigenfunction pair (λ, w) is

$$\alpha\, w_{xxxx} - \beta\,(x w_{xx} + w_x) = \lambda\, w_{xx} \,, \tag{38}$$

$$w(0) = w_{xx}(0) = 0 \,, \quad w(1) = w_{xx}(1) = 0 \,. \tag{39}$$

By solving c_0 from (37), we see that the largest eigenvalue $\lambda_{\max}$ corresponds to the minimal critical velocity.

It is easy to show that all eigenvalues $\lambda \leq 0$. Inserting λ in (37) into (16), we obtain

$$-\alpha \int_0^1 w_{xx} v_{xx} \, \mathrm{d}x - \beta \int_0^1 x w_x v_x \, \mathrm{d}x = \lambda \int_0^1 w_x v_x \, \mathrm{d}x \,. \tag{40}$$

Denote $a(w,v) = -\alpha \int_0^1 w_{xx} v_{xx} \, \mathrm{d}x - \beta \int_0^1 xwv \, \mathrm{d}x$. Choosing $v = w$, we have $a(w,w) \leq 0$, but on the other hand $a(w,w) = \lambda \int_0^1 w_x^2 \, \mathrm{d}x$. Thus $\lambda \leq 0$, and a physically meaningful solution ($c_0^2 > 0$, by (37)) always exists. Furthermore, we see that $c_0^2 \geq 1$, i.e., the critical velocity cannot be smaller than that of a travelling string (for which it is $\sqrt{T_0/m}$).

We apply the Fourier–Galerkin method to problem (38)–(39). Once we have the eigenvalue λ, we can obtain V_0^* from (37) and (8).

We present function w as a Galerkin series (32) in the basis (33). The basis (33) fulfills the boundary conditions (39) naturally. Inserting (33)–(34) into (40), we obtain the matrix equation

$$(-\alpha\,\mathbf{A} - \beta\,\mathbf{B})\,\mathbf{v} = \lambda\,\mathbf{C}\mathbf{v}. \tag{41}$$

Table 1. Physical parameters for the reference case.

g	T_0	m	ℓ	h	E	ν
9.81 m/s^2	500 N/m	0.08 kg/m^2	1 m	10^{-4} m	10^9 N/m^2	0.3

$$\Rightarrow \boxed{\begin{array}{c} D = Eh^3/(12 \cdot (1-\nu^2)) \\ \hline 9.1575 \cdot 10^{-5} \text{ Nm} \end{array}}$$

The elements of matrices in (41) are given in (36).

Equation (41) now becomes a standard generalized linear eigenvalue problem for the pair $(\lambda, \mathbf{v})$, to which any standard solver may be applied.

Numerical results

The physical parameters used are given in Table 1. The number of basis functions used was $n_0 = 200$. By equations (9) and (10), the given values lead to the nondimensional parameter values $\alpha = 1.8315 \cdot 10^{-7}$, $\beta = 1.5696 \cdot 10^{-3}$ and $a_0 = \beta/\alpha = 8.5700 \cdot 10^3$, which was used as a reference case. Problem (35) was solved using the Matlab Optimization Toolbox. Optimization method was chosen to be the interior point method. The results given by optimizer were validated by comparing to solutions given by the direct solver (Fourier–Galerkin method).

Figure 3 presents the buckling modes and the corresponding critical velocities for the different values of a in the case of the Rayleigh–Ritz and the Fourier–Galerkin methods. In each figure, a solid line corresponds to the solution given by the optimizer, and a dash-dot line corresponds to the critical mode given by the differential equation solver. The buckling modes and the critical velocities (in figure titles) were the same in the results given by the optimizer and the direct solver. (The solution plots for the calculated buckling modes overlap.)

Some qualitative observations were made. First, the effect of gravity on the eigenmode is very large, see Figures 3 and 4. The extremum of the eigenmode concentrates toward the start of the span in both studied models. This result is as expected, because positive x axis was chosen to point up in the gravitational field.

The effect of the gravity on the critical velocity is very minor, typically less than 0.01%. See Figure 5. In this respect, the results resemble those from our earlier study, where the effect of a linear tension profile to the buckling behaviour of an axially moving plate was investigated [4].

Furthermore, the strength of the concentration effect depends on the ratio of the dimensionless parameters β and α, i.e. on the quantity $a = \beta/\alpha = mg\ell^3/D$. The larger this parameter is, the stronger is the effect. In the limit $a \to 0$, the effect vanishes. In the other limit $a \to \infty$, the eigenmode approaches a characteristic shape that resembles a sawtooth function (but starts smoothly from 0). See Figure 4.

In the case of nonvertical direction of motion with respect to the gravity, the buckling problem was solved for different values of the angle θ in equation (4). In Figure 6 on the left, the graphs of the buckled shapes are shown for the values $\theta = 0,\ \pi/8,\ ,\pi/4,\ 3\pi/8,\ \pi/2$, and the displacement maxima are marked by $\star$.

In Figure 6 on the right, the buckling modes are represented for the values $[0, \pi/2]$ of θ as a colour sheet. It is seen that the buckling mode rapidly becomes nonsymmetric, when

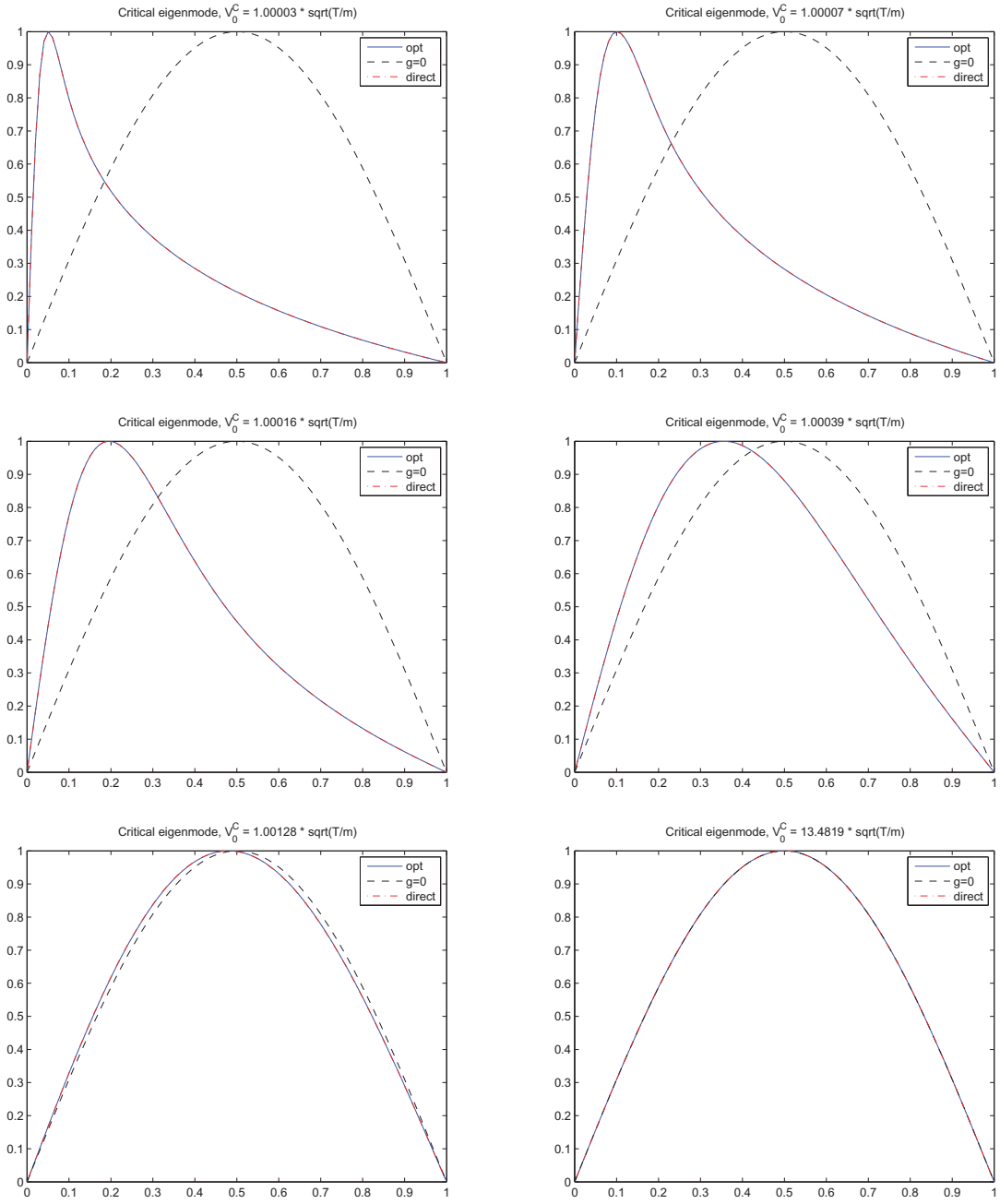

Figure 3. Critical buckling mode for some values of the parameters. The band moves toward the right and gravity points toward the left. Comparison of the solutions given by the energy minimization ("opt", solid line) and by the direct solving of a differential equation ("direct", dash-dot line). The dashed line corresponds to a reference solution with no gravity ($g = 0$).
The top right picture represents the reference case given in the text, for which $a = 8.57 \cdot 10^3$.
In the pictures, $a/a_0 = 10$, 1, 0.1, 0.01, 0.001, 10^{-8} (from left to right, top to bottom, in that order).

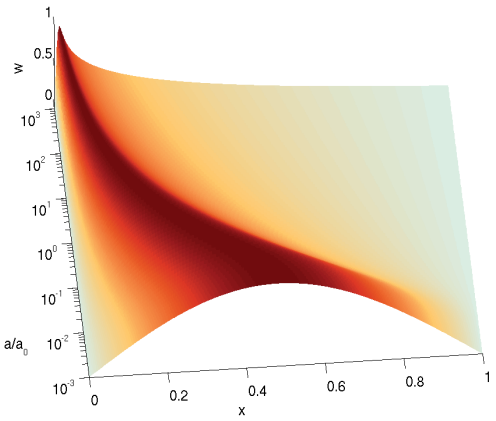

Figure 4. Critical buckling mode for different parameter values. The band moves toward the right and gravity points toward the left.
The reference value is $a_0 = 8.57 \cdot 10^3$. Note the logarithmic scale of a/a_0.

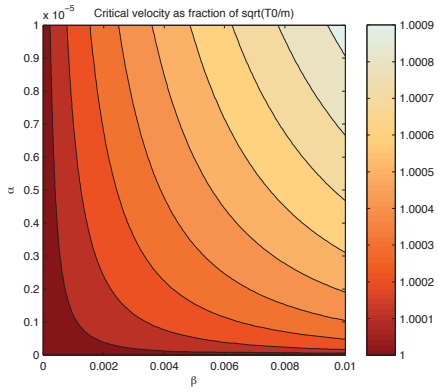

Figure 5. Effect of the dimensionless parameters α and β (defined by (9) and (10)) on the critical velocity. Note that the reference case is at the lower edge of the figure at $\beta \approx 0.0016$. The scaling for the axes was chosen to show the structure of the data.

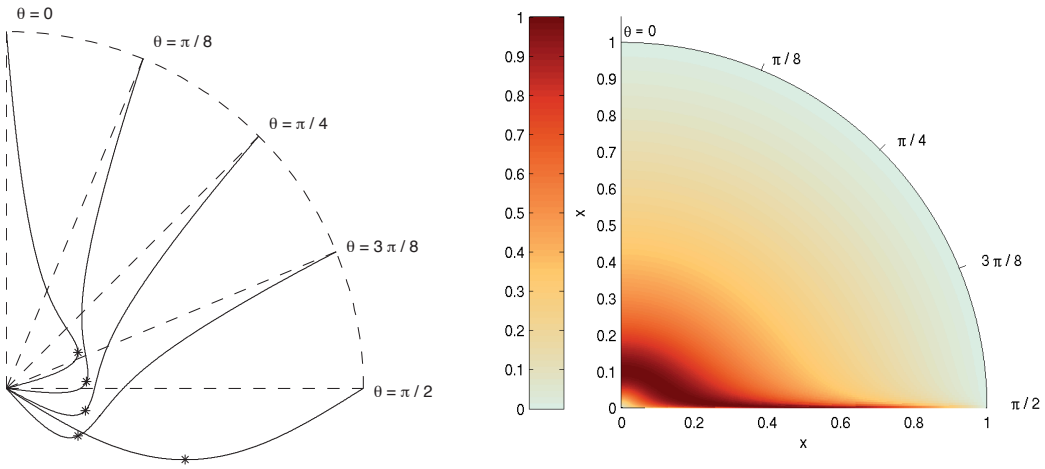

Figure 6. Buckling modes, when the direction of motion of the band is at an angle to the gravity. Left: Graphs of buckling modes for some selected cases. Displacement maxima are marked by $\star$. Right: Colour sheet of the buckling mode for values of θ between 0 and $\pi/2$.

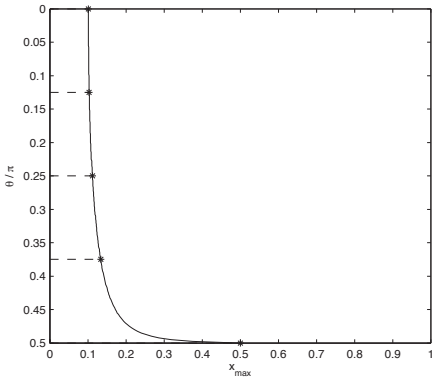

Figure 7. The location of the maximum displacement for θ in $[0, \pi/2]$. The stars ($\star$) correspond to those shown in Figure 6.

the moving direction of the panel non-orthogonal to the gravity, and the nonsymmetric modes are quite similar for small values of θ. This behaviour is illustrated more clearly in Figure 7.

Note that the sign of the axial velocity V_0 does not affect the buckling problem (5)–(6). Therefore, the range $\theta \in [0, \pi/2]$ covers all possible band orientations with respect to the gravity.

Conclusion

The loss of elastic stability of an axially moving band (panel) was investigated, taking the gravitational force into account. The studies performed were mainly based on analytical approaches. The onset of instability in a divergence (static) form for some critical value of the transport velocity was estimated using a variational principle to develop variational inequalities. Analytical lower and upper bounds for the critical velocity were derived. Additionally, it was shown that a critical velocity always exists.

Nonsymmetric solutions of the buckling problem (divergence forms and corresponding critical eigenvalues) were illustrated with the help of numerical examples. As a result, a large influence of the gravity force on the buckling mode, and a small effect on the critical transport velocity, were established and discussed.

Optimization methods were shown to give reliable results for solving this type of differential equations. However, the used interior point method was seen to be slow compared to the direct solver.

The effect of the angle of the motion of the band with respect to the gravity was numerically illustrated. This was done by solving the buckling problem, and the obtained buckling modes were illustrated. Compared to the case where the gravity is orthogonal to the axial motion, and does not affect the buckling mode, it was seen that even a small angle is enough to produce a notably nonsymmetric shape.

Comparing to the effect of introducing a linear tension profile in the noncylidrical deformation case (see [4]), it seems that very high sensitivity of the buckling mode, and very low sensitivity of the critical velocity, to various aspects of the problem setup is a phenomenon typical to this class of problems.

References

[1] F. R. Archibald and A. G. Emslie. The vibration of a string having a uniform motion along its length. *ASME Journal of Applied Mechanics*, 25:347–348, 1958.

[2] N. Banichuk, J. Jeronen, M. Kurki, P. Neittaanmäki, T. Saksa, and T. Tuovinen. On the limit velocity and buckling phenomena of axially moving orthotropic membranes and plates. *International Journal of Solids and Structures*, 48(13):2015–2025, 2011.

[3] N. Banichuk, J. Jeronen, P. Neittaanmäki, and T. Tuovinen. Static instability analysis for travelling membranes and plates interacting with axially moving ideal fluid. *Journal of Fluids and Structures*, 26(2):274–291, 2010.

[4] N. Banichuk, J. Jeronen, P. Neittaanmäki, T. Tuovinen, and T. Saksa. Theoretical study on travelling web dynamics and instability under a linear tension distribution. Technical Report 1, University of Jyväskylä, 2010.

[5] S. Chonan. Steady state response of an axially moving strip subjected to a stationary lateral load. *Journal of Sound and Vibration*, 107:155–165, 1986.

[6] R. Courant and D. Hilbert. *Methods of mathematical Physics*, volume I. Interscience Publishers, Inc., New York, 1966.

[7] T. Frondelius, H. Koivurova, and A. Pramila. Interaction of an axially moving band and surrounding fluid by boundary layer theory. *Journal of Fluids and Structures*, 22(8):1047–1056, 2006.

[8] C. C. Lin. Stability and vibration characteristics of axially moving plates. *International Journal of Solids and Structures*, 34(24):3179–3190, 1997.

[9] C. C. Lin and C. D. Mote. Equilibrium displacement and stress distribution in a two-dimensional, axially moving web under transverse loading. *ASME Journal of Applied Mechanics*, 62:772–779, 1995.

[10] A. C. J. Luo and C. D. Jr. Mote. An exact, closed-form solution for equilibrium of traveling, sagged, elastic cables under uniformly distributed loading. *Communications in Nonlinear Science & Numerical Simulation*, 5(1):6–11, 2000.

[11] W. L. Miranker. The wave equation in a medium in motion. *IBM Journal of Research and Development*, 4:36–42, 1960.

[12] C. D. Mote. Divergence buckling of an edge-loaded axially moving band. *International Journal of Mechanical Sciences*, 10:281–195, 1968.

[13] C. D. Mote. Dynamic stability of axially moving materials. *Shock and Vibration Digest*, 4(4):2–11, 1972.

[14] C. D. Mote. Stability of systems transporting accelerating axially moving materials. *ASME Journal of Dynamic Systems, Measurement, and Control*, 97:96–98, 1975.

[15] Changho Shin, Jintai Chung, and Wonsuk Kim. Dynamic characteristics of the out-of-plane vibration for an axially moving membrane. *Journal of Sound and Vibration*, 286(4-5):1019–1031, September 2005.

[16] A. Simpson. Transverse modes and frequencies of beams translating between fixed end supports. *Journal of Mechanical Engineering Science*, 15:159–164, 1973.

[17] R. D. Swope and W. F. Ames. Vibrations of a moving threadline. *Journal of the Franklin Institute*, 275:36–55, 1963.

[18] A. G. Ulsoy and C. D. Mote. Analysis of bandsaw vibration. *Wood Science*, 13:1–10, 1980.

[19] A. G. Ulsoy and C. D. Mote. Vibration of wide band saw blades. *ASME Journal of Engineering for Industry*, 104:71–78, 1982.

[20] Y. Wang, L. Huang, and X. Liu. Eigenvalue and stability analysis for transverse vibrations of axially moving strings based on hamiltonian dynamics. *Acta Mech Sinica*, 21:485–494, 2005.

[21] J. A. Wickert and C. D. Mote. Classical vibration analysis of axially moving continua. *ASME Journal of Applied Mechanics*, 57:738–744, 1990.

Nikolay Banichuk
Institute for problems in mechanics, Russian Academy of Sciences
Prospekt Vernadskogo 101, 119526 Moscow, Russia
banichuk@ipmnet.ru

Juha Jeronen, Tytti Saksa, Tero Tuovinen
University of Jyväskylä
P.O. Box 35 (Agora), 40014 University of Jyväskylä, Finland
juha.jeronen@jyu.fi, tytti.saksa@jyu.fi, tero.tuovinen@jyu.fi